

WCAP-14310
Revision 2

AP600 DESIGN CERTIFICATION PROGRAM
SPES-2 TESTS FINAL DATA REPORT

L. Conway
R. Hundal
M. Loftus
V. Merrit
M. Ogrinsh

May 1997

WESTINGHOUSE ELECTRIC CORPORATION
Energy Systems Business Unit
P.O. Box 355
Pittsburgh, Pennsylvania 15230-0355

©1997 Westinghouse Electric Corporation
All Rights Reserved

2.6 Facility Operation

The day before the test, SPES-2 personnel verify that:

- the plant is configured for the test
- all plant alarms and protection functions are operating
- the DAS test procedure can perform the required trips for the test
- all the control systems and auxiliary systems are operating
- the plant is ready for start-up

On the day of the test, several key steps are performed to bring the plant up to initial conditions.

The pressurizer internal heaters are turned on and the ADS-1 valve is opened until the primary system fluid temperature reaches 100°C, after which the level and pressure controls are set to auto mode. When primary pressure is about 3 bar, the RCPs are started up. After the rod-bundle electric resistance check (it should be ~1.9 mΩ), the 4 MW power group is turned on to give approximately 60 percent of the maximum current (equivalent to ~900 kW of generated power). The heat-up and pressurization of the facility is carried out maintaining this power until the hot leg temperature reaches 200°C, while subcooling conditions in the circuits. Steam generator levels are brought close to the nominal value and the power channel power is increased step-by-step using the 8 MW and 4 MW power groups. When nominal conditions are reached, they are maintained for about 500 seconds before starting the transient. To start the transient for all tests, a specific break valve (or valves if required) is opened to begin break flow. At this point, the transient follows a course of events that is specific to the test procedure for that particular matrix test.

However, some generalities of the sequence of events for facility operation can be made for most of the tests. Once a setpoint is reached initiating the R signal, the main steam line isolation valves are closed and the power decay simulation (discussed in Section 2.5.1) is begun. Upon S signal initiation, the CMT isolation valves and the PRHR isolation valves are opened, and the main feedwater (MFW) isolation valves are closed, all with a 2-second delay. 16.2 seconds after S signal, the RCP coastdown is initiated. ADS-1 is actuated on CMT volume of 67 percent with the other ADS stages following the delay time specified in the test procedure. Heat loss compensation is terminated with ADS stage 1 actuation. The accumulators begin injecting when the primary system pressure falls to ~700 psia. The IRWST begins injecting water when the primary system pressure is 26 psia. The test is terminated when final conditions are achieved as specified in the test procedure. The specific facility operation and configuration for each test is discussed in subsections 2.6.1 through 2.6.13.

2.6.1 Facility Operation for Test S00303

The purpose of test S00303 was to investigate the plant behavior and system response during a simulated 2 in. cold-leg break on loop B (the CMT side of the plant) with intervention of the passive safety systems only. The test was performed with the pressurizer to CMT-A/B balance lines closed by means of blind flanges installed on both the pressurizer and CMT connections. The break was located at the bottom of loop B cold leg-B2 between the cold leg-B2 to CMT-B balance line and the power channel. The break line for the facility was configured as shown in Figure 2.6-1 with a break orifice installed as described in Figure 2.6.1-2. The orifices installed throughout the facility are listed in Table 2.6.1-1.

Once the facility was at initial conditions, the test was initiated by opening the break valve. When the reactor trip R occurred (pressurizer pressure P-027P = 12.41 MPa = 1800 psia), the heater rod bundle power was controlled to match the scaled AP600 decay heat, and the steam generator MSLIVs were closed with a 2-second delay. When the S signal occurred (pressurizer pressure P-027P = 11.72 MPa = 1700 psia), the PRHR isolation valves and the CMT injection valves were opened and the MFWIVs were closed, all with a 2-second delay, and the RCP coastdown was initiated with a 16.2-second delay.

The CVCS, NRHR, and SFW were off throughout the whole transient. The test simulated the failure of one of two 4th-stage ADS valves on loop B. The ADS valves were programmed to open versus either CMT level L-A40E or L-B40E with the delay time shown in Table 2.6.1-2. The accumulators were set to inject water via DVI when the primary pressure was lower than 4.9 MPa (710.6 psia). The IRWST was set to inject water via DVI when the primary pressure was lower than 0.18 MPa (26.1 psia). The test was terminated when the flow rates (F-A60E/F-B60E) discharged by the IRWST reached a stable flow (without significant fluctuation).

2.6.4 Facility Operation for Test S00605

The purpose of test S00605 was to investigate the asymmetric CMT performance with operation of the PRHR in conjunction with a simulated 2-in. DVI-B break (the CMT side of the plant) and passive safety systems only for mitigation. The break is located on DVI-B between the ECCS injection and the power channel. The test was performed with the pressurizer to CMT A/B balance lines closed by means of blind flanges installed on both the pressurizer and CMT connections. The break line for the facility was configured as shown in Figure 2.6.4-1 with a break orifice installed as described in Figure 2.6.4-2. The other orifices installed throughout the facility are listed in Table 2.6.4-1.

Once the facility was at initial conditions, the test was initiated by opening the break valve. When the reactor trip R occurred (pressurizer pressure P-027P = 12.41 MPa = 1800 psia), the heater rod bundle power was controlled to match the scaled AP600 decay heat, and the steam generator MSLIVs were closed with a 2-second delay. When the S signal occurred (pressurizer pressure P-027P = 11.72 MPa = 1700 psia), the PRHR isolation valves and the CMT injection valves were opened and the MFWIVs were closed, all with a 2-second delay, and the RCP coastdown was initiated with a 16.2-second delay.

The CVCS, NRHR, and SFW were off throughout the whole transient. The test simulated the failure of 1 of 2 fourth-stage ADS valves on loop B. The ADS valves were programmed to open versus either CMT level L-A40E or L-B40E with the delay time shown in Table 2.6.4-2. The accumulators were set to inject water via DVI when the primary pressure was lower than 4.9 MPa (710.6 psia). The IRWST was set to inject water via DVI when the primary pressure was lower than 0.18 MPa (26.1 psia). The test was terminated when the flowrates (F-A60E/F-B60E) discharged by the IRWST reached a stable flow (without significant fluctuation).

TABLE 2.6.4-1
SPES-2 INSTALLED ORIFICES

Location	Diameter (mm)	Thickness (mm)
ADS-1	4.37	12
ADS-2	9.35	12
ADS-3	9.35	12
ADS-4A	20.68	7
ADS-4B	14.62	7
CMT-A injection line	4.1	5.5
CMT-B injection line	5.7	5.5
CMT-A cold leg bal. line (2 orif.)	7.5	5.5
CMT-B cold leg bal. line (2 orif.)	7.5	5.5
Accumulator-A injection line	4.86	7.3
Accumulator-B injection line	4.86	7.3
DVI-B break device	2.56	3.3 *

* Rounded entrance with 2.6 mm radius

**TABLE 2.6.6-1
SPES-2 INSTALLED ORIFICES**

Location	Diameter (mm)	Thickness (mm)
ADS-1	3.09	12
ADS-2	9.35	12
ADS-3	6.61	12
ADS-4A	20.68	7
ADS-4B	20.68	7
CMT-A injection line	4.1	5.5
CMT-B injection line	5.7	5.5
CMT-A cold leg bal. line (2 orif.)	7.5	5.5
CMT-B cold leg bal. line (2 orif.)	removed	-
Accumulator-A injection line	4.86	7.3
Accumulator-B injection line	4.86	7.3
CL-BL-B break device CMT side	8.95 **	9 *
CL-BL-B break cold leg side	8.71	9 *

* Rounded entrance with 9 mm radius (see Figures 2.6.6-2 and 2.6.6-3)

** The actual scaled break size of the 8-inch Sch. 160 CL-BL is 8.71 mm. However, since no significant amount of break flow is discharged from this point, the 8.95 mm orifice from matrix test No. 6 was utilized (see Figure 2.6.6-3).

**TABLE 2.6.6-2
PROGRAMMED OPENING OF ADS VALVES**

ADS Stage	Orifice Dia. (mm/in.)	CMT Volume (%)	L-A40E or L-B40E (m/ft.)	Delay Time (sec.)
First	3.09/0.122	67	4.152/13.622	30
Second	9.35/0.368	67	4.152/13.622	125
Third	6.61/0.260	67	4.152/13.622	245
Fourth A	20.68/0.814	20	1.192/3.911	60 sec after 20% CMT vol., but no sooner than 360 sec. after 67% CMT vol.
Fourth B	20.68/0.814	20	1.192/3.911	60 sec after 20% CMT vol., but no sooner than 360 sec. after 67% CMT vol.

**TABLE 2.6.9-1
SPES-2 INSTALLED ORIFICES**

Location	Diameter (mm)	Thickness (mm)
ADS-1	4.37	12
ADS-2	9.35	12
ADS-3	9.35	12
ADS-4A	20.68	7
ADS-4B	14.62	7
CMT-A injection line	4.1	5.5
CMT-B injection line	5.7	5.5
CMT-A CL bal. line (2 orif.)	7.5	5.5
CMT-B CL bal. line (2 orif.)	7.5	5.5
Accumulator-A injection line	4.86	7.3
Accumulator-B injection line	4.86	7.3
SG-B tube break device	0.85	5 *

* Rounded entrance with 0.9 mm radius

TABLE 2.6.9-2
PROGRAMMED OPENING OF ADS VALVES

ADS Stage	Orifice Dia. (mm/in.)	CMT Volume (%)	L-A40E or L-B40E (m/ft.)	Delay Time (sec.)
First	4.37/0.172	-	-	2 min + 30 sec after "S"
Second	9.35/0.368	-	-	2 min + 125 sec after "S"
Third	9.35/0.368	-	-	2 min + 245 sec after "S"
Fourth A	20.68/0.814	20	1.192/3.911	0 sec after 20% CMT vol., but no sooner than 360 sec after 67%
Fourth B	14.62/0.576	20	1.192/3.911	60 sec after 20% CMT vol., but no sooner than 360 sec after 67%

TABLE 2.6.10-1
SPES-2 INSTALLED ORIFICES

Location	Diameter (mm)	Thickness (mm)
ADS-1	2.2	12
ADS-2	9.35	12
ADS-3	2.2	12
ADS-4A	20.68	7
ADS-4B	14.62	7
CMT-A injection line	4.1	5.5
CMT-B injection line	5.7	5.5
CMT-A cold leg bal. line (2 orif.)	7.5	5.5
CMT-B cold leg bal. line (2 orif.)	7.5	5.5
Accumulator-A, injection line	4.86	7.3
Accumulator-B injection line	4.86	7.3
SG-B tube break device	0.85	5 *
* Rounded entrance with 0.9 mm radius		

**TABLE 2.6.10-2
PROGRAMMED OPENING OF ADS VALVES**

ADS Stage	Orifice Dia. (mm/in.)	CMT Volume (%)	L-A40E or L-B40E (m/ft.)	Delay Time (sec.)
First	2.2/0.072	67	4.152/13.622	30
Second	9.35/0.368	67	4.152/13.622	125
Third	2.2/0.072	67	4.152/13.622	245
Fourth A	20.68/0.814	20	1.192/3.911	60 sec after 20% CMT vol., but no sooner than 360 sec. after 67% CMT vol.
Fourth B	14.62/0.576	20	1.192/3.911	60 sec after 20% CMT vol., but no sooner than 360 sec. after 67% CMT vol.

2.6.11 Facility Operation for Test S01512

Test S01512, a large steam line break with passive safety systems only, was simulated using the steam generator-A PORV as the break opening. The steam generator-A PORV had an orifice installed with a diameter of 20.4 mm (shown in Figure 2.6.11-1) which corresponds to an AP600 break area of 1.388 ft². (This area corresponds to the steam generator outlet nozzle orifice area.) The other orifices installed at the facility are listed in Table 2.6.11-1.

Test S01512 was performed with the facility operating at full pressure and flow, but at "hot standby" conditions. The power channel was at zero power (i.e., no decay heat was simulated) but with heater rod power at 150 kW for facility heat loss compensation. Additionally, the following initial conditions existed:

- RCPs were running at nominal flow (cold leg flow = 12.92 lb/sec.)
- pressurizer pressure was at 2250 psia
- core ΔT was $\sim 1^\circ\text{F}$ ($T_{\text{avg}} = 545^\circ\text{F}$)
- pressurizer level was between 6.56 ft. and 8.2 ft.
- steam generators pressure was approximately 1000 psi
- steam generators narrow range level was approximately 4.9 ft.
- main feedwater isolation valves were closed
- common steam line isolation valve (BV-07) was closed
- main steam isolation valves (BV-05A/BV-05B) were opened
- CVCS, NRHR, and SFW were not operational.

The test was initiated by opening the steam generator-A PORV (BV-06A) at time zero. All heat loss compensation was terminated when the steam generator-A PORV was opened. Based on pretest predictions using a lead/lag function of 50/5, the S signal was manually generated by the SPES plant computer one second after the break opening. The pressurizer internal heaters were shut off by the S signal. Also, at S signal, the CMT and PRHR isolation valves were opened with a two-second delay, the main steam line isolation valves were closed with a 4-second delay, and the RCPs were shutdown with a 16.2-second delay.

The ADS was not expected to actuate for this test, but was programmed to open versus CMT level with the appropriate time delays as listed in Table 2.6.11-2. The accumulators were pressurized to inject when the primary pressure was reduced to less than 696 psia. The IRWST was at full normal level such that it would inject water when the primary pressure was lower than 26.1 psia. The test was terminated when the primary system temperatures and pressures had stabilized and the CMT level was not decreasing.

**TABLE 2.6.11-1
SPES-2 INSTALLED ORIFICES**

Location	Diameter (mm)	Thickness (mm)
ADS-1	4.37	12
ADS-2	9.35	12
ADS-3	9.35	12
ADS-4A	20.68	7
ADS-4B	20.68	7
CMT-A injection line	4.1	5.5
CMT-B injection line	5.7	5.5
CMT-A CL bal. line (2 orif.)	7.5	5.5
CMT-B CL bal. line (2 orif.)	7.5	5.5
Accumulator-A injection line	4.86	7.3
Accumulator-B injection line	4.86	7.3
Steamline-A break device	20.4	10 *

* Rounded entrance with 5 mm radius

**TABLE 4.1.2-3
SPES-2 HOT PRE-OPERATIONAL TEST H-01 MAJOR COMPONENT HEAT LOSSES**

Flow rate in each cold leg = 0.619 kg/sec.
Total power = 142.6 kW

Component	Component Metal Mass lbm ⁽¹⁾	Component Heat Capty. (Btu/°F)	Inlet Average Temperature (°F)	Outlet Average Temperature (°C)	Heat Losses (kW)	Heat Loss Percentage due to the Component (%)
PC/HL (A&B)						
RCP-A/ CL-A1,A2						
RCP-B/ CL-B1,B2						
SG-A						
SG-B						
Total Heat Losses =					[]	(a,b,c)

Notes:

- (1) The weight of these components does not include flange and bolting metal masses.
- (2) These data are not relevant for the calculation of steam generator heat losses, as their metal heat capacity contribution can be neglected.
- (3) Pump power released to the fluid at low flow can be neglected.
- (4) The difference between total power and total heat losses is due to the heat capacity of the system.

TABLE 4.1.2-4
SPES2 PRE-OPERATIONAL TEST H-01 FACILITY SYSTEM HEAT CAPACITIES

Source File	Time Interval ⁽¹⁾ (sec.)	Temperature Linear Increase (°C)	Total Power Input Rate ⁽²⁾ (kW)	Calculated Heat Losses (kW)	Calculated Heat Capacity (kJ/°C)
acqdat_spes.dat;242					
acqdat_spes.dat;242					
acqdat_spes.dat;244					
Average Heat Capacity =					8480

(a,b,c)

Notes:

- (1) This time interval is considered valid for the value of data recorded.
- (2) The total power includes pump heat power released to fluid:

Pump A = kW
 Pump B = kW

**TABLE 4.1.2-5
SPES-2 HOT PRE-OPERATIONAL TEST H-05
INITIAL CONDITIONS**

Condition	Specified	Actual
Pressurizer pressure	500.5 psig (24.9 bar)	
Pressurizer level	12.4 ft. (3.78 m)	
Hot-leg temperature	415.6°F (213.1°C)	
Cold-leg temperature	---	
Power (kW)	192.3	
Upper-head flow rate	0.40 lb/sec. (0.18 kg/sec.)	
Steam generator pressure	270.6 psig (18.66 bar)	
Steam generator level	>36.2 ft. (>11.02 m)	
Accumulator pressure	197 psig (13.59 bar)	
Accumulator level	6.86 ft. (2.09 m)	
IRWST level	28 ft. (8.53 m)	
Cold-leg/CMT balance line temperature	Cold-leg temperature	
CMT external vessel	not pressurized	
PRHR supply line temperature	302°F (150°C)	
Pressurizer Cold-leg balance line	>437.9°F (>225.5°C)	

drained at this time (data plots 20 through 23) and did not affect the rest of the test. The accumulator injection was initiated when the primary system pressure dropped below []^(a,b,c) psia prior to ADS-1 actuation. However, the injection rate was low (less than []^(a,b,c) lbm/sec.) due to the small difference between the primary system and accumulator pressures (data plot 39).

Facility Response During the PDP:

The system response during the PDP was almost identical to that of test S00303, with the exception that ADS-1 occurred []^(a,b,c) seconds later in this test S00504.

The oscillating flow that was observed in the tubular downcomer and in the rod bundle following the RCP coastdown continued into the PDP. The flow oscillations resulted in large oscillations of the steam fraction of the two-phase mixture exiting the rod bundle and flowing into the hot legs (data plots 30 and 31). These oscillations in steam fraction had a significant effect on the thermal buoyancy head that drove the flow through the primary system at this time. The fluid steam fraction oscillations were observed through the hot leg and the steam generators (data plots 20 and 21). However, the two-phase mixture entering the steam generators left the steam generators as saturated water (data plots 24 through 27). Some of the steam was condensed in the U-tubes (the primary-side pressure was higher than the secondary-side pressure at this time, allowing some heat to be transferred to the secondary-side fluid). The remaining steam was separated from the two-phase mixture in the high point of the U-tubes due to the low velocity, which eventually caused the U-tubes to begin to drain. For steam generator-A, primary system flow continued until 210 seconds into the transient, then intermittent flow was observed through steam generator-A (plots 20 and 22). This was caused by the oscillations in the steam fraction where the buoyancy head in the hot leg was high enough to spill over the top of the U-tubes at the peaks of the oscillating buoyancy head. At approximately []^(a,b,c) seconds ([]^(a,b,c) seconds), all flow through the steam generators ended since the free-water surface in the U-tubes had fallen too low to be overcome by the buoyancy head oscillations. These oscillations were seen in temperatures and pressures throughout the primary system. When the cold-leg side of the steam generator U-tubes were completely drained (about []^(a,b,c) seconds), these oscillations stopped.

The primary system pressure decrease during the PDP began at a slow rate of []^(a,b,c) psi/sec. At approximately []^(a,b,c) seconds into the event, the primary system pressure decay rate increased to []^(a,b,c) psi/sec. This happened when the CMTs transitioned from their recirculation mode of operation to their draindown mode. This transition occurred when the B-loop cold legs partially drained and the CMT balance lines drained. This resulted in a higher CMT injection rate (Figure 4.2.4-1). The increased rate of pressure decay in the primary system was due to the increased injection rate of the cold liquid from the CMTs (occurred at different times for the two CMTs).

The CMTs began injecting cold fluid into the annular downcomer []^(a,b,c) seconds after the S signal occurred. Initially, this injection was by natural circulation at approximately 0.12 lbm/sec. through each CMT, with hot fluid flowing from the cold leg through the cold-leg balance line

(CLBL) into the top of the CMT, and cold fluid flowing from the bottom of CMT. Between []^(a,b,c) seconds (data plot 38), CMT-A transitioned to draindown mode when cold leg-B2 partially drained and subsequently the cold-leg balance line (CLBL) for CMT-A drained, and a free-water surface developed in the top of the CMT-A as the level started to drop (data plot 33). The CMT injection flow, when draindown began, increased to approximately 0.28 lbm/sec. and gradually decreased as the CMT level decreased (reducing the driving head). See data plot 38.

For CMT-B the transition from recirculation to draindown occurred at approximately []^(a,b,c) seconds (earlier than for CMT-A), and its injection flow increased to approximately []^(a,b,c) lbm/sec. and gradually decreased.

The free-liquid surfaces in the CMTs were established by steam flowing from the cold legs to the CMTs through the CLBLs. The steam flow from the cold legs condensed in the CMTs and heated the free-water surface. For CMT-A, the CMT water surface was heated by the steam to saturation temperature (data plot 15) and flashing could occur as the pressure decreased in the system.

Both the recirculation and draindown modes of CMT operation established a stable thermal gradient in the CMT water. The CMT water maintained a stable thermal stratification throughout its operation.

The accumulators began to inject fluid into annular downcomer via the DVI lines when system pressure dropped below []^(a,b,c) psia (at approximately []^(a,b,c) seconds). However, the injection rate was very low prior to ADS-1 (data plot 39).

Throughout the PDP, the PRHR removed energy from the primary system. However, the combined effect of the PRHR cooling the primary fluid and the cold injection flow from the CVCS and CMTs was sufficient to limit the steam fraction of the two-phase fluid flowing through the rod bundle and rod bundle cooling was maintained during this phase (data plots 30 and 31).

- **Automatic Depressurization System Phase ([]^(a,b,c) Seconds to End Of Test)**

The automatic depressurization system (ADS) phase began with the actuation of ADS-1 and continued until the end of the transient (Figure 4.2.4-1).

Facility Response During the ADS Phase:

With the actuation of ADS-1, followed by ADS-2 and ADS-3 within approximately []^(a,b,c) seconds, the rate of system depressurization increased from []^(a,b,c) psi/sec. at the end of the PDP to []^(a,b,c) psi/sec. at the start of the ADS phase. This rate gradually decreased as system pressure decreased.

steam from the two-phase mixture from the hot leg at the low-flow velocities existing at natural circulation flow conditions. The fluid level on the hot-leg side of the U-tubes oscillated as it decreased. This condition continued until approximately []^(a,b,c) seconds into the transient, at which time the top of the U-tubes remained filled with saturated vapor and the U-tube water level decreased smoothly.

The fluid level on the cold-leg side of the steam generator-A U-tubes exhibited significant level oscillations from about []^(a,b,c) seconds and it appeared that intermittent flow over the top of the U-tubes occurred. At []^(a,b,c) seconds, the U-tube water level decreased smoothly and was drained at about []^(a,b,c) seconds.

Because of the higher steam fraction of the fluid in hot leg-B and steam generator-B, the time over which oscillations occurred was reduced and the U-tubes filled with saturated vapor sooner. As a result, the steam generator-B U-tubes began to drain at about []^(a,b,c) seconds.

The level in the steam generator-B hot-leg side U-tubes dropped to near zero at about []^(a,b,c) seconds. The cold-leg side U-tubes exhibited significant level oscillations from about []^(a,b,c) seconds which continued until the U-tubes were drained at []^(a,b,c) seconds (data plots 22 and 23).

• Hot Legs

Hot legs-A and -B were full of two-phase fluid until ADS-1 was actuated, when the measured level decreased (data plots 20 and 21). The hot legs were nearly drained at ADS-4 ([]^(a,b,c) seconds) and partially refilled after IRWST injection began. The principal difference between hot legs-A and -B was the influence of the PRHR HX on the void fraction in the hot legs during the PDP. Assuming that the fluid in the hot legs initially had the same steam fractions at the outlet of the power channel lower-upper plenum, the PRHR appeared to have preferentially removed steam from hot leg-A (as seen in the very high steam fraction for the PRHR inlet flow)—thereby reducing the steam fraction of the fluid in hot leg-A to less than the fluid steam fraction in hot leg-B. The apparent steam fraction in hot leg-A was []^(a,b,c) percent at []^(a,b,c) seconds; while in hot leg-B it was []^(a,b,c) percent. The hot-leg steam fraction affected the draining of the steam generators U-tubes, with steam generator-B draining earlier than steam generator-A.

• Cold Legs

Cold legs-A1 and -A2 remained full until []^(a,b,c) seconds (data plots 22 through 27), at which time the level decreased to the horizontal section of the pipes and drained at about []^(a,b,c) seconds. When ADS-4 occurred, the water level in the tubular downcomer temporarily dropped reaching []^(a,b,c) ft. below the hot-leg elevation at []^(a,b,c) seconds (data plot 24). The rod bundle steam fraction fluid increased. After IRWST injection began at []^(a,b,c) seconds, the annular downcomer refilled and the cold and hot legs were partially refilled after []^(a,b,c) seconds to the level of []^(a,b,c) ft. above the hot leg.

Cold legs-B1 and -B2 remained full until approximately []^(a,b,c) seconds into the event, at which time both cold legs-B1 and -B2 drained rapidly to the level of the horizontal section of the pipes. This reduced water level in cold leg-B1 and cold leg B-2 initiated the transition of the CMTs from their recirculation to draindown mode of operation. Cold legs-B1 and -B2 were refilled at []^(a,b,c) seconds to the level of []^(a,b,c) ft. above the hot leg. At this time, the cold leg to CMT balance lines were partially filled.

• PRHR and IRWST

At the initiation of the test, the PRHR HX was filled with subcooled liquid. When the S signal occurred, the PRHR HX isolation valve opened and flow started through the HX at a high flow rate due to the still operating RCPs. When the RCPs were shutoff and the power channel upper plenum and the hot legs filled with two-phase fluid, a large portion of the steam in hot leg-A flowed to the PRHR HX (data plot 29). The two-phase mixture, consisting of alternating slugs of steam and water, was condensed and subcooled in the PRHR HX (data plot 28) from []^(a,b,c)°F to below []^(a,b,c)°F. During the PDP (prior to ADS-1), there was a significant variation in the flow through the PRHR HX, caused by the variation in the steam fraction in hot leg-A. Steam condensation was apparently occurring in the PRHR HX as evidenced by the rapid and wide variations in dP measurements (data plots 28, 29, and 37).

When ADS-1 began, the power channel and the hot leg were refilled with subcooled water by accumulator injection. The driving head for the flow in the PRHR HX decreased (caused by the density difference between the fluid in the PRHR supply line and the return line) and the flow decreased and stopped. There was a short period of reverse flow at the end of the accumulator discharge. The subcooled fluid in the hot leg never filled the PRHR supply line, and hot fluid in this line flashed as system pressure decreased. Simultaneous flashing in the supply line and condensation in the PRHR HX resulted in a wide variations in the measured flow in the PRHR HX return line.

After the accumulator injection had ended, the rod bundle upper plenum again reached saturation temperature, and a two-phase mixture again occurred in the hot legs. Flow restarted in the PRHR HX, and the flow rate varied in response to the steam fraction in the hot leg. When ADS-4 fully depressurized the primary system and the IRWST flow began and refilled the power channel and the hot leg with subcooled water again, the flow through the PRHR HX stopped for the remainder of the transient. The subcooled fluid in the hot leg filled the PRHR supply line at []^(a,b,c) seconds.

Following ADS-4, primary system pressure decreased to near ambient, and gravity flow due to the water elevation head in the IRWST began injecting water into the annular downcomer via the DVI lines. The flow from the IRWST was sufficient to refill the power channel, downcomer, and loop piping and to establish subcooled fluid flow through the tube bundle and out through the ADS-4 flow paths (data plots 32 and 40).

• Core Makeup Tanks

The CMT injection was initiated two seconds after the S signal when the CMT injection line isolation valves were opened. Initially, the flow from the CMTs occurred by natural circulation; hot water from cold legs flowed to the top of the CMTs and cold water from the bottom of the CMTs flowed to the downcomer, via the DVI lines, into the power channel.

Initially, this recirculation rate was approximately 0.13 lbm/sec. from each CMT. The flow rate slowed down to []^(a,b,c) lbm/sec. at []^(a,b,c) seconds due to the decreased buoyant head driving force that occurred as the CMT water was replaced with hot water from the cold legs, and as the cold-leg water temperature decreased.

After cold legs-B1 and -B2 drained to the level of horizontal pipes at approximately []^(a,b,c) seconds, flashing/draining began in the cold-leg balance line. When the temperature at the top of the CMT reached the saturation temperature for primary system pressure, a free-water surface was established in the CMTs. This increased the driving head for the injection flow and resulted in a higher draindown flow rate. For the 1-inch LOCA, the break flow at this time was less than full CMT draindown flow rate. This caused the CMT injection to consist intermittent short periods of draindown, which increased the cold-leg water level and short periods of refill with water from the cold legs. This resulted in a slow decrease in CMT levels and the ADS-1 actuation was therefore delayed and occurred at a system pressure of approximately []^(a,b,c) psia, considerably below 711 psia accumulator gas pressure. Part of the accumulator coolant inventory was therefore injected into the primary system prior to ADS-1. This accumulator injection helped maintain the primary system coolant inventory at cold-leg elevation and thus contributed to intermittent CMT draindown/refill. For test S00401, the break was located in cold leg-B2, resulting in cold leg-B2 draining before cold leg-B1. Since the CMT-B balance line was connected to cold leg-B2, the draindown began earlier for CMT-B (at 2170 to 2450 seconds) than for CMT-A (at []^(a,b,c) seconds), as shown in data plot 38. The CMT balance lines finally completely drained at []^(a,b,c) seconds (ADS-1), resulting in an increase in CMT injection flow rate. The steam in the CMT balance lines and at top of the CMTs was slightly superheated as the primary system pressure was rapidly reduced by ADS operation.

The CMTs were heated first by the hot liquid which replaced the cold water draining from the bottom of the CMTs. A stable, stratified thermal gradient was established in the CMTs (data plots 15 and 16). Later steam from the cold legs maintained the exposed metal and free-water surface temperatures at or near saturation temperature.

The CMT recirculation mode flow rate was initially approximately []^(a,b,c) lbm/sec. and steadily decreased to approximately []^(a,b,c) lbm/sec. when the transition to draindown began. The CMT average injection flow rate increased to approximately []^(a,b,c) lbm/sec. during the transition period. After ADS-1 actuated, CMT injection increased again to []^(a,b,c) lbm/sec. and then gradually decreased with time. During the accumulator injection (ADS-1), the CMTs' draindown rate remained high. CMT-A was drained at about ADS-4 ([]^(a,b,c)

seconds). The CMT-B injection flow rate decreased when the IRWST started at about []^(a,b,c) seconds, and CMT-B drained at []^(a,b,c) seconds (data plot 33).

- **Accumulators**

The accumulators provided water injection by a polytropic expansion of a compressed air volume stored within the accumulator. Accumulator injection started when the primary system pressure dropped below 711 psia at []^(a,b,c) seconds. The accumulator injection flow rate was low until ADS-1 was actuated at approximately []^(a,b,c) seconds when the flow rate increased to approximately []^(a,b,c) lbm/sec. The accumulator injection after ADS actuation lasted approximately []^(a,b,c) seconds, and the accumulators were completely drained (data plot 34).

The effective polytropic coefficient of expansion was calculated for the accumulators (Figures 4.2.5-3 and 4.2.5-4) to be []^(a,b,c) for accumulator-A and []^(a,b,c) for accumulator-B. This was near the mid-point between isothermal expansion ($k = 1$) and adiabatic expansion ($k = 1.4$) and showed that some heat was picked up by the compressed air from the internal metal surfaces of the accumulator during the expansion.

Mass Discharge and Mass Balance

The catch tank weight measurements are shown in data plot 43 for the break flow, for the ADS-1, -2, and -3 flows, and for the ADS-4 flow. The break flow as shown in plot 44, which began when the test was initiated, decreases as system pressure drops during the IDP and the PDP. When the ADS was actuated, the break location voided, and further discharge from the break was primarily saturated steam until IRWST injection refilled the cold leg after ADS-4.

The discharge from ADS-1, -2, and -3 was stable throughout the accumulator injection and increased temporarily when the injection ended. When ADS-4 occurred, the discharge of fluid from the top of the pressurizer essentially ended, and the fluid discharge from ADS-4 began. The ADS-4 fluid discharge rate was relatively stable and continued until the end of the test. The discharged masses are shown in Table 4.2.5-4.

The mass balance results for test S00401 were calculated based on water inventory before and after the test. Table 4.2.5-2 gives a detailed listing of the inventories of water in the various components before the test. Table 4.2.5-3 lists the inventories after the test and the amount of water injected into the vessel from the IRWST. The water level in the vessel was determined by the DP-B16P measurement to be []^(a,b,c) in. []^(a,b,c) above the hot-leg centerline at the end of the test. Table 4.2.5-4 compares the mass balance for the system before and after the test and shows 98.5% agreement of the measurements.

4.2.6 One-In. Cold-Leg Break with Three PRHR HX Tubes, without Nonsafety Systems (S01613)

This matrix test was performed to be identical to matrix test S00401 with the exception that the number of PRHR HX tubes in use was increased from 1 tube to 3 tubes. This test simulated a 1-in. break in the bottom of cold leg-B2. The test began with the initiation of the break in cold leg-B2, which was the cold leg with the CMT-B pressure balance line connection. The break location was just downstream from the cold leg to the core makeup tank (CMT) balance line connection. This test was performed without any nonsafety systems (chemical and volume control system [CVCS] makeup pumps, steam generator startup feedwater [SFW] pumps, and normal residual heat removal system [NRHR] pumps) operating.

Results are provided in the data plot package at the end of this section. The sequence of events for S01613 is listed in Table 4.2.6-1.

The AP600 SPES-2 tests were marked by distinctly different phases. These phases were characterized by the rate at which the primary system pressure decreased and the thermal-hydraulic phenomena occurring within the primary and safety systems. The different phases selected for the purpose of detailed evaluation of this LOCA are shown in Figure 4.2.6-1 and are as follows:

- Initial depressurization phase (IDP)—Point 1 to 2
- Pressure decay phase (PDP)—Point 2 to 3
- Automatic depressurization system (ADS) phase—Point 3 to 4
- Post-automatic depressurization system (post-ADS) phase—Point 4 to 5

Overall Test Observations

Figure 4.2.6-1 shows the plant primary system pressure during test S01613 (as measured at the top of the pressurizer), with selected component actuations and plant responses shown in relation to primary system pressure.

The IDP began with the initiation of the break, which resulted in a rapid reduction in pressure. The reactor trip (R) signal initiated at 1800 psia. The safety systems actuation (S) signal initiated at 1700 psia. The R and the S signals initiated the following actions:

- Decay power simulation (with heat loss compensation) initiated
- Main steamline isolation valves (MSLIVs) closed
- Main feedwater isolation valves (MFWIVs) closed
- CMT injection line isolation valves opened
- Passive residual heat removal (PRHR) return line isolation valve opened
- Reactor coolant pumps (RCPs) stopped running

Recirculation flow through the CMTs and flow through the PRHR heat exchanger (HX) began immediately after their isolation valves opened. Flashing/boiling occurred in the rod bundle and

upper-plenum regions of the power channel due to the rapid decrease in primary pressure to the fluid saturation pressure. The measured fluid level in the upper-upper plenum decreased to the hot-leg elevation. The flashing on the hot-leg side of the primary system stopped the rapid drop in primary system pressure. When the RCPs were shut off (at []^(a,b,c) seconds), the flow through the rod bundle began to oscillate (with a []^(a,b,c)-second period). This resulted in oscillations in the rod bundle and lower-upper plenum collapsed liquid level and fluid temperature, and system pressure.

During the initial stages of the PDP, the rod bundle collapsed liquid level decreased (fluid steam fraction increased). This caused an increasing steam fraction in the upper plenum and the hot legs. The hot leg-B fluid had a steam fraction close to that observed in the upper plenum. The steam fraction in hot leg-A was lower due to the selective removal of vapor from the hot leg into the PRHR HX inlet line.

Two-phase flow in the hot legs initiated draining of the steam generator U-tubes, as steam from the two-phase mixture collected in the top of the U-tubes. This stopped the primary system flow through the steam generators so that the power channel flow was composed predominantly of the flow through the PRHR HX. The steam fraction oscillations observed in the rod bundle and in the upper plenum ended when the steam generator U-tubes drained. Approximately []^(a,b,c) seconds into the test, the steam generator-B U-tubes began to drain. The steam generator-A U-tubes began to drain, approximately []^(a,b,c) seconds later due to the lower fluid steam fraction in hot leg-A.

Due to boiling in the rod bundle (data plots 30 and 31), two-phase flow entered the hot leg from the upper plenum and flowed through the PRHR HX. The flow into the PRHR HX consisted of intermittent periods of saturated water and steam which had an average steam fraction significantly greater than the fluid in the upper plenum. The average steam fraction at the PRHR HX inlet was as high as []^(a,b,c) percent, which enhanced the PRHR HX heat transfer from the primary system, as compared to its heat removal capability with single-phase saturated or subcooled water. When the primary system flow stabilized after the initial flow oscillations, a PRHR HX heat removal rate of []^(a,b,c) kW was calculated. This calculation was based on the steam fraction at the PRHR HX inlet (as calculated from the dP instrument readings in data plot 29), the averaged return flow rate, the HX inlet and outlet temperatures, and the pressure. This calculation, which assumes a slip coefficient of 1 between water and steam, may be lower than the actual heat transfer and should only be used for test-to-test comparison.

When the primary system pressure decreased to the saturation pressure for the fluid in the upper head, it began to drain (at approximately []^(a,b,c) seconds).

When the loop-B cold legs had partially emptied, the CMTs transitioned from their recirculation mode of operation to an intermittent draindown mode of operation at approximately []^(a,b,c) seconds.

During the first []^(a,b,c) seconds of this test (shortly after ADS-1 actuation), []^(a,b,c) lbm of water were expelled through the break draining the: the pressurizer, the steam generator U-tubes, the power channel upper head, the power channel upper plenum above the hot leg, most of the cold legs,

and approximately []^(a,b,c) percent of the CMTs. The heated rods that simulate the AP600 core decay heat reduced power to approximately 230 kW at 4800 seconds. This value consisted of 80-kW of decay heat and 150-kW of heat loss compensation. The mass flow rate out of the break was decreasing, indicating that cold leg-B2 was almost empty.

The ADS phase began with the actuation of ADS-1 (at approximately []^(a,b,c) seconds). ADS-2 and -3 occurred within the next []^(a,b,c) seconds. The heat loss compensation was removed from the rod bundle power decay simulation when ADS-1 occurred, reducing the rod bundle power to approximately 80 kW.

The ADS actuation increased the rate of primary system depressurization and resulted in high injection flow from the accumulators. The rapid injection of cold water from the accumulators (from []^(a,b,c) seconds) and the CMT injection flow refilled the power channel/upper plenum, the horizontal portion of the hot legs and the pressurizer. When the accumulator discharge ended, the flow through the heater bundle decreased to the injection rate of the CMTs and the PRHR HX flow, and two-phase flow occurred again the heater bundle, hot leg-A, the PRHR HX, and into the pressurizer. The rod bundle steam fraction continued to increase (collapsed liquid level decreased) until after ADS-4 was actuated.

The mass flow rate through the break decreased sharply at approximately []^(a,b,c) seconds, indicating that cold leg-B2 emptied and that the break flow was steam. During the ADS phase, approximately []^(a,b,c) lbm of subcooled water were discharged from ADS-1, -2, and -3.

The post-ADS period began when ADS-4 actuated. ADS-4 occurred at []^(a,b,c) seconds, the fluid discharge through ADS-1, -2, and -3 stopped, and the pressurizer water drained back into hot leg-A. A small amount of CMT flow continued into the downcomer via the direct vessel injection (DVI) line. When the primary system pressure decreased below the pressure corresponding to the water elevation head of the IRWST, flow from the IRWST began. Shortly thereafter, the CMT flow ended. The flow from the IRWST gradually refilled and subcooled the power channel, restored single-phase water flow through the rod bundle, and partially refilled the upper-upper plenum. The PRHR HX supply line partially emptied at approximately []^(a,b,c) and the PRHR HX was no longer effective. A steady flow of subcooled water was established from the IRWST into the downcomer, through the power channel, and left the primary system through the ADS-4 flow paths.

This test demonstrated that the heater bundle was fully covered by a single- or two-phase fluid at all times during this test (data plots 30 and 31). There was no indication of heater rod temperature increase due to lack of cooling (data plot 3). Key parameters comparing the S01613 test with other tests are listed in Table 5-1 in Section 5.0.

Discussion of Test Transient Phases

- **Initial Depressurization Phase (0 to []^(a,b,c) Seconds)**

The initial depressurization phase (IDP) began with the initiation of the break (at time 0) and ended when the primary system pressure reached the saturation pressure of the fluid in the lower-upper plenum and the hot legs (Figure 4.2.6-1). This phase included the following events: R signal at 1800 psia (decay power simulation initiated and the MSIV closed), and S signal at 1700 psia (the MFWIV closed, the CMT injection line isolation valves opened, and the PRHR heat exchanger return line isolation valve opened—all with a 2-second delay; and RCP coastdown started after a 16.2-second delay). See Table 4.2.6-1.

Facility Response During the IDP:

From time 0 until the R signal occurred, the primary system pressure decreased due to the expansion of the pressurizer steam volume caused by fluid loss through the break. The pressurizer partially compensated for the loss of pressure by flashing; however, it was drained after []^(a,b,c) seconds (data plot 32). The R (at []^(a,b,c) seconds) and the S (at []^(a,b,c) seconds) signals were based on pressurizer pressure only. When the R signal occurred, the MSLIV closed and the power was reduced to 20 percent of full power after a 5.75-second delay and began to decay after a 14.5-second delay.

As a result of the power reduction without flow reduction, the rod bundle ΔT decreased due to the low power/flow ratio and the lower-upper plenum temperature dropped toward the cold-leg temperature. At the same time, the primary system pressure had decreased to []^(a,b,c) psia (the saturation pressure of the []^(a,b,c)°F water in the upper-upper plenum), and the upper-upper plenum began to flash and rapidly drain. System pressure decreased to approximately []^(a,b,c) psia at []^(a,b,c) seconds. At this time, the pressurizer was drained, but primary system pressure was still dictated by the temperature of the saturated vapor in the pressurizer (about []^(a,b,c)°F) and the fluid in the surge line. When the RCPs shut off (at []^(a,b,c) seconds), the rod bundle and upper-plenum fluid temperatures increased due to the increased power/flow ratio at the lower flow. System pressure increased temporarily until the decreasing rod bundle decay power and the decreasing lower-plenum temperature (due to the CMTs injecting cold water into the downcomer) began to reduce the lower-upper plenum fluid temperature. The decrease in primary system pressure resulted from the balance between the steam generation rate (from flashing primary fluid), the volumetric flow of liquid out of the break, and the steam condensation occurring in the PRHR HX. Steam was continually generated by boiling due to the heater power. As system pressure continued to decrease, more fluid reached its saturation pressure and flashed. The PRHR HX flow started before the RCPs were tripped and then continued by natural circulation (data plot 37). Primary system pressure stabilized at saturation pressure for the bulk hot fluid in the primary system (approximately 540°F), as shown in Figure 4.2.6-1. This ended the IDP.

The flow oscillations in the hot legs reached the steam generators. In steam generator-A, the U-tubes were full until approximately []^(a,b,c) seconds into the transient. At this time, a free-water surface began to develop in the top of the U-tubes, primarily due to the separation of steam from the two-phase mixture from the hot leg at the low-flow velocities existing at natural circulation flow conditions. The fluid level on the hot-leg side of the U-tubes oscillated as it decreased. This condition continued until approximately []^(a,b,c) seconds into the transient, at which time the top of the U-tubes remained filled with saturated vapor and the U-tube water level decreased smoothly.

The fluid level on the cold-leg side of the steam generator-A U-tubes exhibited significant level oscillations from about []^(a,b,c) seconds and it appeared that intermittent flow over the top of the U-tubes occurred. At []^(a,b,c) seconds, the U-tube water level decreased smoothly and was drained at about []^(a,b,c) seconds.

Because of the higher steam fraction of the fluid in hot leg-B and steam generator-B, the time over which oscillations occurred was reduced and the U-tubes filled with saturated vapor sooner. As a result, the steam generator-B U-tubes began to drain at about []^(a,b,c) seconds.

The level in the steam generator-B hot-leg side U-tubes dropped to near zero at about []^(a,b,c) seconds. The cold-leg side U-tubes exhibited significant level oscillations from about []^(a,b,c) seconds which continued until the U-tubes were drained at []^(a,b,c) seconds (data plots 22 and 23).

• Hot Legs

Hot legs-A and -B were full of two-phase fluid until ADS-1 was actuated, when the measured level decreased (data plots 20 and 21). The hot legs were nearly drained at ADS-4 ([]^(a,b,c) seconds) and partially refilled after IRWST injection began. The principal difference between hot legs-A and -B was the influence of the PRHR HX on the void fraction in the hot legs during the PDP. Assuming that the fluid in the hot legs initially had the same steam fractions at the outlet of the power channel lower-upper plenum; the PRHR appears to have preferentially removed steam from hot leg-A (as seen in the very high steam fraction for the PRHR inlet flow), thereby reducing the steam fraction of the fluid in hot leg-A to less than the fluid steam fraction in hot leg-B. The apparent steam fraction in hot leg-A was []^(a,b,c) percent at []^(a,b,c) seconds; while in hot leg-B it was []^(a,b,c) percent. The hot-leg steam fraction affected the draining of the steam generators U-tubes, with steam generator-B draining earlier than steam generator-A.

• Cold Legs

Cold legs-A1 and -A2 remained full until []^(a,b,c) seconds (data plots 22 through 27), at which time the level decreased to the horizontal section of the pipes and drained at about []^(a,b,c) seconds. When ADS-4 occurred, the water level in the tubular downcomer temporarily dropped reaching []^(a,b,c) ft. below the hot-leg elevation at []^(a,b,c) seconds (data plot 24). The rod

bundle steam fraction fluid increased. After IRWST injection began at []^(a,b,c) seconds, the annular downcomer refilled and the cold and hot legs were partially refilled after []^(a,b,c) seconds to the level of []^(a,b,c) ft. above the hot leg.

Cold legs-B1 and -B2 remained full until []^(a,b,c) seconds into the event, at which time both cold legs-B1 and -B2 drained rapidly to the level of the horizontal section of the pipes. This reduced water level in cold leg-B1 and cold leg B-2 initiated the transition of the CMTs from their recirculation to draindown mode of operation. Cold legs-B1 and -B2 were refilled at []^(a,b,c) seconds to the level of []^(a,b,c) ft. above the hot leg. At this time, the cold leg to CMT balance lines were partially filled.

• PRHR and IRWST

At the initiation of the test, the PRHR HX was filled with subcooled liquid. When the S signal occurred, the PRHR HX isolation valve opened and flow started through the HX at a high flow rate due to the still operating RCPs. When the RCPs were shutoff and the power channel upper plenum and the hot legs filled with two-phase fluid, a large portion of the steam in hot leg-A flowed to the PRHR HX (data plot 29). The two-phase mixture, consisting of alternating slugs of steam and water, was condensed and subcooled in the PRHR HX (data plot 28) from []^(a,b,c)°F to below []^(a,b,c)°F. During the PDP (prior to ADS-1), there was a significant variation in the flow through the PRHR HX, caused by the variation in the steam fraction in hot leg-A. Steam condensation was apparently occurring in the PRHR HX as evidenced by the rapid and wide variations in dP measurements (data plots 28, 29, and 37).

After the ADS sequence began, the power channel and the hot legs were refilled with subcooled water by accumulator injection. The driving head for flow through the PRHR HX decreased due to the sharp decrease in the PRHR HX supply line temperature (data plot 19) and the flow decreased.

After accumulator injection flow decreased, the upper plenum and hot leg-A again became saturated (data plots 4 and 5), and a two-phase mixture again occurred in the hot legs; the PRHR HX supply line began to drain; and PRHR HX flow rapidly decreased and essentially stopped. In spite of the increasing steam fraction of the fluid in the rod bundle and upper plenum that occurred prior to IRWST injection, PRHR HX flow did not restart.

The heatup of IRWST water resulting from the operation of the PRHR HX is shown in data plot 17. Following ADS-4, primary system pressure decreased to near ambient, and gravity flow due to the water elevation head in the IRWST began injecting water into the annular downcomer via the DVI lines. The flow from the IRWST was sufficient to refill the power channel, downcomer, and loop piping and to establish subcooled fluid flow through the tube bundle and out through the ADS-4 flow paths (data plots 32 and 40).

• Core Makeup Tanks

The CMT injection was initiated two seconds after the S signal when the CMT injection line isolation valves were opened. Initially, the flow from the CMTs occurred by natural circulation; hot water from cold legs flowed to the top of the CMTs and cold water from the bottom of the CMTs flowed to the downcomer, via the DVI lines, into the power channel.

Initially, this recirculation rate was approximately []^(a,b,c) lbm/sec. from each CMT. The flow rate slowed down to []^(a,b,c) lbm/sec. at []^(a,b,c) seconds due to the decreased buoyant head driving force that occurred as the CMT water was replaced with hot water from the cold legs, and as the cold-leg water temperature decreased.

After cold legs-B1 and -B2 drained to the level of horizontal pipes at []^(a,b,c) seconds, flashing/draining began in the cold-leg balance line. When the temperature at the top of the CMT reached the saturation temperature for primary system pressure, a free-water surface was established in the CMTs. This increased the driving head for the injection flow and resulted in a higher draindown flow rate. For the 1-inch LOCA, the break flow at this time was less than full CMT draindown flow rate. This caused the CMT injection to consist intermittent short periods of draindown which increased the cold leg water level and short periods of refill with water from the cold legs. This resulted in a slow decrease in CMT levels and the ADS-1 actuation was therefore delayed and occurred at a system pressure of approximately []^(a,b,c) psia, considerably below 711 psia accumulator gas pressure. Part of the accumulator coolant inventory was therefore injected into the primary system prior to ADS-1. This accumulator injection helped maintain the primary system coolant inventory at cold-leg elevation and thus contributed to intermittent CMT draindown/refill. For test S01613, the transition from recirculation to the draindown mode of operation occurred at []^(a,b,c) seconds for both CMT A and CMT B as shown in data plot 38. The CMT balance lines finally completely drained at []^(a,b,c) seconds (ADS-1), resulting in an increase in CMT injection flow rate. The steam in the CMT balance lines and at top of the CMTs was slightly superheated as the primary system pressure was rapidly reduced by ADS operation.

The CMTs were heated first by the hot liquid from the which replaced the cold water draining from the bottom of the CMTs. A stable, stratified thermal gradient was established in the CMTs (data plots 15 and 16). Later steam from the cold legs maintained the exposed metal and free-water surface temperatures at or near saturation temperature.

The CMT recirculation mode flow rate was initially approximately []^(a,b,c) lbm/sec. and steadily decreased to approximately []^(a,b,c) lbm/sec. when the transition to draindown began. The CMT average injection flow rate increased to approximately []^(a,b,c) lbm/sec. during the transition period. After ADS-1 actuated, CMT injection increased again to []^(a,b,c) lbm/sec. and then gradually decreased with time. During the accumulator injection (ADS-1), the CMTs' draindown rate remained high. CMT-A was drained at about ADS-4 ([]^(a,b,c) seconds). The CMT-B injection flow rate decreased when the IRWST started at about []^(a,b,c)

seconds, and CMT-B stopped flowing at []^(a,b,c) seconds and never completely drained (data plots 33 and 38).

- **Accumulators**

The accumulators provided water injection by a polytropic expansion of a compressed air volume stored within the accumulator. Accumulator injection started when the primary system pressure dropped below 711 psia at 2400 seconds. The accumulator injection flow rate was low until ADS-1 was actuated at approximately []^(a,b,c) seconds when the flow rate increased to approximately []^(a,b,c) lbm/sec. The accumulator injection after ADS actuation lasted approximately []^(a,b,c) seconds, and the accumulators were completely drained (data plot 34).

The effective polytropic coefficient of expansion was calculated for the accumulators (Figures 4.2.5-3 and 4.2.5-4) to be []^(a,b,c) for accumulator-A and -B. This was near the midpoint between isothermal expansion ($k = 1$) and adiabatic expansion ($k = 1.4$) and showed that some heat was picked up by the compressed air from the internal metal surfaces of the accumulator during the expansion.

Mass Discharge and Mass Balance

The catch tank weight measurements are shown in data plot 43 for the break flow, for the ADS-1, -2, and -3 flows, and for the ADS-4 flow. The break flow as shown in plot 44, which began when the test was initiated, was stable with a decreasing flow rate as system pressure dropped during the IDP and the PDP. When the ADS was actuated, the break location voided, and further discharge from the break was primarily saturated steam until IRWST injection refilled the cold leg after ADS-4.

The discharge from ADS-1, -2, and -3 was stable throughout the accumulator injection and increased temporarily when the injection ended. When ADS-4 occurred, the discharge of fluid from the top of the pressurizer essentially ended, and the fluid discharge from ADS-4 began. The ADS-4 fluid discharge rate was relatively stable and continued until the end of the test. The discharged masses are shown in Table 4.2.6-4.

The mass balance results for test S01613 were calculated based on water inventory before and after the test. Table 4.2.6-2 gives a detailed listing of the inventories of water in the various components before the test. Table 4.2.6-3 lists the inventories after the test and the amount of water injected into the vessel from the IRWST. The water level in the vessel was determined by the DP-B16P measurement to be []^(a,b,c) in. (577 mm) above the hot-leg centerline at the end of the test. Table 4.2.6-4 compares the mass balance for the system before and after the test and shows 102.6% agreement of the measurements.

**TABLE 4.2.6-1
SEQUENCE OF EVENTS FOR TEST S01613**

Event	Specified	Instrument Channel	Actual Time (sec.)
Break Opens	0	Z_001BC	(a,b,c)
R Signal	P = 1800 psia	P-027P	
MSL IV Closure	R signal + 2 sec.	Z_A04SO, F_A04S	
		Z_B04SO, F_B04S	
SCRAM	R signal + 5.7 sec.		
S Signal	P = 1700 psia	P-027P	
CMT IV Opening	S signal + 2 sec.	Z_A040EC, F-A40E	
		Z_B040EC, F-B40E	
PRHR Heat Exchanger Actuation	S signal + 2 sec.	Z_A81EC, F_A80E	
MFW IV Closure	S signal + 2 sec.	Z_B02S0, F_B01S	
		Z_A02S0, F_A01S	
Reactor Coolant Pumps Tripped	S signal + 16.2 sec.	DP-A00P	
		DP-B00P	
Accumulators	P-027P = 710 psia	F_A20E	
	+30 sec.	Z_001PC	
ADS-2	CMT level 67%	L_B40E	
		+125 sec.	Z_002PC
ADS-3	CMT level 67%	L_B40E	
		+245 sec.	Z_003PC
ADS-4 A/B	CMT level 20%	L_B40E	
		+60 sec.	Z_004PC, F-040P
IRWST Injection	P-027P = 26 psia	F_A60E	
		F_B60E	

**TABLE 4.2.6-2
WATER INVENTORY BEFORE TEST S01613**

PRIMARY SYSTEM					
Component	Volume (ft.³)/(l)	Net Vol (ft.³)/(l)	Temp (°F)	Relative Density	Mass (lbm)
Loops	8.97 ft. ³ (254.0 l)	8.97 ft. ³ (254.0 l)			
Pressurizer	3.37 ft. ³ (95.4 l)	1.82 ft. ³ (51.6 l)			
Surge Line	0.34 ft. ³ (9.6 l)	0.34 ft. ³ (9.6 l)			
Tubular Downcomer	1.38 ft. ³ (39.1 l)	1.38 ft. ³ (39.1 l)			
Annular Downcomer + High-Pressure Bypass	0.54 ft. ³ (15.3 l)	0.54 ft. ³ (15.3 l)			
Core Bypass	0.44 ft. ³ (12.4 l)	0.44 ft. ³ (12.4 l)			
Lower Plenum	0.81 ft. ³ (22.8 l)	0.81 ft. ³ (22.8 l)			
Riser	1.64 ft. ³ (46.4 l)	1.64 ft. ³ (46.4 l)			
Upper Plenum	1.46 ft. ³ (41.3 l)	1.46 ft. ³ (41.3 l)			
Upper Head	1.90 ft. ³ (53.8 l)	1.90 ft. ³ (53.8 l)			
CMT-A	5.05 ft. ³ (143.0 l)	5.05 ft. ³ (143.0 l)			
CMT-B	5.05 ft. ³ (143.0 l)	5.05 ft. ³ (143.0 l)			
ACC-A	5.05 ft. ³ (143.0 l)	3.90 ft. ³ (110.4 l)			
ACC-B	5.05 ft. ³ (143.0 l)	3.90 ft. ³ (110.4 l)			
IRWST Injection Line	0.18 ft. ³ (5.1 l)	0.18 ft. ³ (5.1 l)			
TOTAL PRIMARY INVENTORY					

(a,b,c)

4.2.12 Steam Generator Tube Rupture without Nonsafety Systems (S01110)

This matrix test simulated a steam generator tube rupture (SGTR) without any nonsafety systems operating or operator actions, and with only the automatic passive safety systems used for accident mitigation. The pressurizer internal heaters were shut-off at break initiation and the chemical and volume control system (CVCS), normal residual heat removal (NRHR) function, and startup feedwater system (SFWS) were shut-off for this test. The single SGTR is simulated via a line connected from the primary side (reactor coolant pump (RCP) B suction piping) to the secondary side of steam generator-A (approximately []^(a,b,c) ft. above the tube sheet), with a break orifice diameter scaled to simulate []^(a,b,c) times the area of a AP600 steam generator tube.

Results are provided in the data plot package at the end of this section. The sequence of events for S01110 is listed in Table 4.2.12-1. During mitigation of the SGTR, there was no core makeup tank (CMT) draindown, and no accumulator or in-containment refueling water storage tank (IRWST) injection throughout the transient.

Since this SGTR test did not result in automatic depressurization system (ADS) actuation only the first two event phases observed in loss-of-coolant accident (LOCA) recovery occurred. The event phases selected for purpose of detailed evaluation of the non-LOCA events are shown in Figure 4.2.12-1 and are as follows:

- Initial depressurization phase (IDP) - Point 1 to 2
- Pressure decay phase (PDP) - Point 2 to 3

Overall Test Observations

Figure 4.2.12-1 shows the facility primary system pressure during matrix test S01110 (as measured at the top of the pressurizer) in relation to selected component actuations and other facility responses.

The IDP began with the opening of the break valve between the primary and secondary side, causing the pressurizer to drain. The pressurizer heaters remained on after break initiation until approximately 250 seconds, slowing the reduction in pressure due to pressurizer steam expansion. After the heaters shut-off, the reactor pressure decreased at a faster rate until the reactor trip and safety system actuation occurred.

When the pressurizer level dropped to []^(a,b,c) ft. at []^(a,b,c) seconds, the reactor trip (R) and safety system actuation (S) signals were actuated. []^(a,b,c) seconds later, the main steam line isolation valves (MSLIVs) and main feedwater isolation valves (MFWIVs) were closed, the CMT and passive residual heat removal (PRHR) heat exchanger (HX) return line isolation valves were opened, and the RCPs coasted down with a []^(a,b,c)-second delay (at []^(a,b,c) seconds into the event). Rod bundle power was reduced to []^(a,b,c) percent of full power after a []^(a,b,c)-second delay (at []^(a,b,c) seconds), and the simulated power decay began after a []^(a,b,c)-second delay. The bundle power was maintained 150 kW above the scaled decay power to compensate for facility heat losses.

The recirculation flow through the CMTs and the PRHR flow began immediately after the isolation valves were opened. The changing rod bundle power to flow ratio caused by the time delays between rod bundle power was reduced. When the RCPs were tripped and coasted down, this reduction caused a sharp decrease, then increase in the hot leg temperature. This reduction also caused a rapid decrease in pressurizer pressure from []^(a,b,c) to []^(a,b,c) psia followed by a slight increase in pressure. Primary pressure then decreased to the steam generator saturation pressure due to heat transfer to the steam generators. The IDP ended at []^(a,b,c) seconds, when hot leg/upper plenum temperature ([]^(a,b,c)°F) started to control the primary system pressure; and break flow stabilized at approximately []^(a,b,c) lb/sec. (Figure 4.2.12-5). Data plot 31 shows that the level of the upper-upper plenum above the hot legs began to decrease.

During the initial portion of the PDP (up to []^(a,b,c) seconds), the primary system, with the exception of the upper-upper plenum and upper head, remained water solid. Primary system cooling was provided by the PRHR HX, CMT recirculation, break flow, and facility heat losses. At []^(a,b,c) seconds, these were 83 kW, 84 kW, 7 kW and approximately 125 kW, respectively (approximately 300 kW total), as compared to the heated rod power of 245 kW at []^(a,b,c) seconds. Thus, the primary and secondary system temperature and pressure slowly decreased throughout the PDP. The above PRHR HX heat removal rate was based on the steam fraction of the flow in the PRHR supply line (calculated to be low at this time, as determined from the dP instrument readings in data plot 29) and the PRHR flow rate, HX inlet and outlet temperatures, and pressure.

As shown in data plot 31, at approximately []^(a,b,c) seconds the upper-upper plenum and the upper head began to drain at a significant rate. This resulted in an increasing pressurizer level (data plot 32). The upper-upper plenum drained rapidly from approximately []^(a,b,c) seconds and was completely drained to the hot leg elevation at approximately []^(a,b,c) seconds.

At this time, primary system and secondary system pressures were essentially equalized and several events occurred almost simultaneously:

- The break flow to steam generator-B decreased from approximately []^(a,b,c) lbm/sec. at []^(a,b,c) seconds to approximately []^(a,b,c) at []^(a,b,c) seconds (Figure 4.2.12-5). Total break flow mass from the primary system to secondary side of steam generator-B was approximately []^(a,b,c) lbm (Figure 4.2.12-3).
- The steam generator-B tubes began to drain at approximately []^(a,b,c) seconds.
- The loop-B cold leg flows decreased and loop-A flows increased momentarily.
- Steam voiding began in the rod bundle resulting in two-phase flow through the lower-upper plenum, hot legs, PRHR supply line, etc.
- The pressurizer level rapidly increased in response to the draining steam generator-B tubes, upper head, and primary system steam generation.

This resulted in oscillations of temperature, steam fraction, tubular downcomer flow, and system pressure, all of which continued throughout the test. The pressurizer was completely filled at []^(a,b,c) seconds and remained filled until the test was terminated. The CMT natural recirculation flow continued, but the flow rate was decreasing. The upper head was completely drained at []^(a,b,c) seconds, and the level never recovered. The primary system pressure oscillated about the secondary system pressure and there was a small alternating flow in the break line.

Due to periodic boiling in the heater rod bundle (data plots 30 and 31), two-phase mixture with wide variations in steam fraction entered the hot leg and flowed to the steam generators and PRHR HX. This resulted in alternating slugs of steam and water in the PRHR HX supply line, which resulted in oscillations in the PRHR heat removal rate and return flow rate. The oscillating return to flow into the cold legs and tubular downcomer caused small heater rod temperature oscillations.

Hot leg-B fluid had a steam fraction close to that in the lower-upper plenum. However, the steam fraction in hot leg-A was lower due to the selective removal of steam from the hot leg into the PRHR inlet line. The steam fraction at the PRHR HX inlet oscillated and reached high peaks, which enhanced the PRHR heat removal from the primary system as compared to the heat removal with single-phase saturated or subcooled water before []^(a,b,c) seconds.

As stated above, the steam generator-B U-tubes began draining at approximately []^(a,b,c) seconds into the event. At the end of the event, the steam generator-B U-tubes were drained, including part of the pump B suction line. The U-tubes steam generator-A never drained; however, there was an oscillating flow with wide variations in steam fraction in the upper section of the U-tubes.

This test demonstrated that the heater rod bundle was fully covered (single-phase or two-phase mixture) at all times during this test (data plots 30 and 31) and that there was no indication of heater rod temperatures increasing due to lack of cooling (data plot 3). Also, the passive safety system functions were shown to mitigate the consequences of a SGTR with no operator actions or use of nonsafety systems. Key parameters comparing the S01110 test with other tests are listed in Table 5-1 in Section 5.0.

Discussion of Test Transient Phases

- **Initial Depressurization Phase (0 to 1050 Seconds)**

The initial depressurization phase (IDP) began with the initiation of the break (at time 0) and lasted until the primary system pressure decreased to the saturation pressure for the upper plenum and the hot legs (Figure 4.2.12-1). This period included the following events: initiation of the break, the actuation of the R and S signals, closure of the MSLIV and MFWIV, opening of the CMT injection line isolation valves, and opening of the PRHR HX return line isolation valve; all with a []^(a,b,c)-second delay. Rod bundle power was reduced to []^(a,b,c) percent with a []^(a,b,c)-second delay, the rod bundle decay power was initiated with a []^(a,b,c) second delay, and RCP coastdown was initiated after a []^(a,b,c)-second delay.

System Response during the IDP:

The break was initiated at time 0. From time 0 until the R and S signals were activated (at []^(a,b,c) seconds), the system lost pressure due to the fluid loss through the break resulting in a decreased pressurizer level and an expansion of the pressurizer steam bubble. When the trip signals were activated, the power was reduced to []^(a,b,c) percent of full power after []^(a,b,c) seconds. At []^(a,b,c) seconds, the SPES-2 integrated power from the time of the R signal simulates the AP600 post-trip integrated power. The SPES-2 power was then decreased to simulate the AP600 decay heat plus 150 kW for facility heat loss compensation, which was maintained throughout this transient. The MSLIV was closed at []^(a,b,c) seconds. As a result of the power reduction without flow reduction, the rod bundle ΔT decreased, and lower-upper plenum temperature dropped temporarily to the lower plenum temperature of []^(a,b,c)°F. The system pressure decreased to []^(a,b,c) psia at []^(a,b,c) seconds (Figure 4.2.12-2). At this time, the pressurizer drained and the system pressure was controlled by the temperature of the saturated fluid ([]^(a,b,c)°F) in the surge line. When the RCPs were shut off (at []^(a,b,c) seconds), the rod bundle and the lower-upper plenum temperatures increased to []^(a,b,c)°F, as a result of the increased power/flow ratio for the rod bundle at the lower flow. The system pressure increased temporarily to []^(a,b,c) psia until there was a drop in the decay power and there was a reduction in the plenum temperature. The lower plenum temperature was affected by the CMT cold fluid injection into the downcomer and the PRHR HX flow into cold leg. The pressure decreased at a rate of []^(a,b,c) psia/sec in this time period (at []^(a,b,c) seconds). The CMT recirculation flow and the PRHR flow, break flow, and facility heat losses were sufficient to keep the flow through the power channel subcooled.

The PRHR flow started before the RCPs were shut off and continued by natural circulation after RCP coastdown (data plot 37). The primary system pressure stabilized at the saturation pressure for the bulk temperature of fluid on the hot-leg side of the power channel (approximately 540°F) at []^(a,b,c) seconds. This ended the IDP.

• Pressure Decay Phase (1050 Seconds to End-of-Test)

The pressure decay phase (PDP) began when the primary system pressure (Figure 4.2.12-2) was dictated by the saturation pressure for the hot-leg fluid temperature, and continued until the end of the test. This phase was characterized by a slow decrease in the overall system pressure and temperature. The rod bundle power (decay power plus heat loss compensation) reduced from []^(a,b,c) kW to []^(a,b,c) kW (data plot 1).

At []^(a,b,c) seconds (bundle power []^(a,b,c) kW), the PRHR HX heat removal rate was approximately []^(a,b,c) kW, the CMTs provided approximately []^(a,b,c) kW effective heat removal due to the cold CMT water replacing the hot water entering the CMTs through the balance lines, the break flow removed approximately []^(a,b,c) kW, and facility heat losses were approximately []^(a,b,c) kW. Thus, the total heat removal exceeded heat input (299 kW versus 245 kW), there was no boiling in the rod bundle, and primary system pressure decreased slowly.

**TABLE D-2
OUT-OF-RANGE AND MODIFIED INSTRUMENTS BY TEST (Cont.)**

TIN	Out-of-Range Instrument	Comments	Instrument "Zero" Out of Specification	Modified Instrument	Reason for Modification	Corrective Action
S00706 (Cont.)	DP-B06P	OOB-HL (41s + 1733s) OOB-HL (2146s + 2204)				
		OOB-HL (2932s + 2965s)				
	DP-B00S	OOB-HL (-300s + 149s)				
	DP-B05S	OOB-HL (-150s + EOT)				
	DP-B20E	OOB-HL (-300s + 16s)				
	DP-B28P	OOB-HL (-300s + 709s)				
		OOB-HL (-300s + 19s)				
		OOB-HL (23s + 506s)				
	DP-B40E	OOB-HL (0s + 622s)				
	DP-B41E	OOB-HL (1s + 41s)				
	DP-B42E	OOB-HL (0s + 30s)				
	DP-B43E	OOB-HL (0s + 41s)				
	DP-B44E	OOB-HL (3s + 23s)				
	DP-B45E	OOB-HL (23s + 413s)				
	F-014P	OOB-HL (22s + EOT)				
	F-A02S	OOB-HL (47s + 1959s)				
	F-A20E	OOB-HL (2339s + 2417s)				
	F-A80E	OOB-HL (531s + 581s)				
	F-B01S	OOB-HL (21 + 43s)				
	F-B20E	OOB-HL (-300 + 17s)				
	OOB-HL (1s + 113s)					
	OOB-HL (325s + 383s)					
	F-B40E	OOB-HL (20 + 140s)				

Note: Out of range for instrument high limit (at least for 2s); OOB-HL = Out of range for instrument low limit (at least for 2s); EOT = End of test.

**TABLE D-2
OUT-OF-RANGE AND MODIFIED INSTRUMENTS BY TEST (Cont.)**

TIN	Out-of-Range Instrument	Comments	Instrument "Zero" Out of Specification	Modified Instrument	Reason for Modification	Corrective Action
S00908	F-A04S	Nozzle pressure drop too high.	DP-B00S (29.3 mV)	DP-000P	Error in SAD database.	Subtract 8.48 kPa to the values. Acquired as T-A02E. Not installed on break line. Not installed on break line.
	F-B04S	Nozzle pressure drop too high.	DP-B05S (-34.3 mV)			
	T-G01A F-001A	Measurement not required.	DP-A06S (-54.4 mV)	T-A021PL	SAD amplifier damaged.	
	T-A02E F-A00E	Measurement not required.	DP-A00S (-63.2 mV)	DE-001PA	Instrument not available.	
	T-B02E F-B90E	Measurement not required.	DP-A04S (-26.5 mV)			
	T-A20A F-A20A	Measurement not required.		DE-001V3	Instrument not available.	
	T-B20A F-B20A	Measurement not required.				
	DP-001P	OOB-LL (965s + 900s)				
	DP-002P	OOB-LL (965s + 1076s)				
	DP-003P	OOB-LL (20s + EOT)				
	DP-018P	OOB-HL (0s + 19s)				
	DP-019P	OOB-LL (0s + 17s)				
	DP-020P	OOB-LL (0s + 9s)				
	DP-A00P	OOB-HL (35s + 45s)				
		OOB-HL (627s + 2628s)				
	DP-A05S	OOB-HL (-300s + 8s)				
	DP-A06P	OOB-LL (1785s + 1802s)				
	DP-A20E	OOB-LL (-300s + 180s)				
	DP-A28P	OOB-LL (-300s + 0s)				
		OOB-HL (1s + 8s)				
		OOB-LL (10s + 98s)				
		OOB-LL (722s + 1122)				
		OOB-LL (1425s + 1691s)				
	DP-A40E	OOB-LL (989s + 992s)				
	DP-A41E	OOB-HL (0s + 20s)				
	DP-A42E	OOB-HL (0s + 27s)				
		OOB-HL (117s + 119s)				
	DP-A44E	OOB-HL (1s + 22s)				
	DP-A82E	OOB-HL (-300s + 26s)				
	DP-A83E	OOB-HL (10s + 29s)				
		OOB-LL (675s + EOT)				
	DP-B00P	OOB-HL (29s + 2651s)				
	DP-B022P	OOB-LL (717s + 986s)				
DP-B05S	OOB-HL (-300s + 8s)					
DP-B20E	OOB-LL (-300s + 183s)					
DP-B28P	OOB-LL (-300s + 0s)					
	OOB-HL (1s + 1675s)					

Note:

Out of range for instrument high limit (at least for 2s); OOB-LL = Out of range for instrument low limit (at least for 2s); EOT = End of test.

E-1 Objectives

The objectives of the error analysis are as follows:

- To describe the errors of the measurements performed during the SPES-2 test program.
- To give the results of the error analysis calculation.

The error analysis was performed in metric units; however, the final results are reported in English units.

E-2 Error Evaluation

During the test, all measured instrumentation data of the primary and secondary circuit were recorded at a sampling frequency of 2.0 Hz. The recorded data were converted to engineering units (SI) and then plotted versus time. The engineering values were also recorded on magnetic tape in order to transmit the data to Westinghouse Electric Corporation.

E-2.1 Direct Measured Quantities

The direct measured quantities (such as absolute pressures, pressure drops, fluid speed, voltages, current, etc.), acquired and recorded by data acquisition system (DAS), were converted into engineering (SI) units using linear formulas:

$$Y = \pm M * (mV - q) \pm K = \pm M * mV + Q$$

where:

- mV = signal coming from instrument
- M, q = calibration constants (q = instrument zero)
- K = instrument hydraulic head = $\rho_{LC} * g * h$
- Q = $\pm M * q \pm K$

and where:

- ρ_{LC} = water density assumed at ambient temperature = 1000 (kg/m³)
- h = pressure tap height difference (m)
- g = acceleration due to gravity = 9.80665 (m/sec.²)

To verify that the instrument will meet the required accuracy for test, the instruments were controlled and calibrated in the laboratory before installation in the facility. In the facility, the instrument was

checked just before the beginning of the experiment in order to control all the IAS recording channels. The instrument zero was verified daily before starting the test.

Temperatures

The temperature of the fluid, piping, components, and in-containment refueling water storage tank (IRWST) pool water were measured in degrees Celsius by using the following:

- Sheated thermocouples type K Chromel-Alumel, 0.5- to 1.5-mm OD
- Resistance thermal detector (RTD) thermoresistances type PT 100

A matrix E (mV), T (°C), for K-type thermocouples was generated by the following formula (UNI-7938 specifications):

$$E = \left(\sum_{(i=1)}^8 d_i T^i + 125 \exp [-1/2 * (T - 127/65)^2] \right) / 1000$$

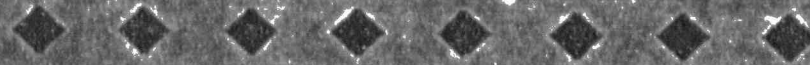
where:

- E = electrical signal (mV)
T = temperature (°C)
d₀ = -1.853306 * 10⁻¹
d₁ = 3.891834 * 10⁻¹
d₂ = 1.664515 * 10⁻²
d₃ = -7.870237 * 10⁻⁵
d₄ = 2.283579 * 10⁻⁷
d₅ = -3.570023 * 10⁻¹⁰
d₆ = 2.993291 * 10⁻¹³
d₇ = -1.284985 * 10⁻¹⁶
d₈ = 2.223997 * 10⁻²⁰

The value of temperature T (°C) was obtained from the signals coming from thermocouples E (mV), performing a linear interpolation of the matrix E, T. In the same way, the signals coming from thermoresistances (Ω) were converted to engineering units (°C) performing the linear interpolation of the PT100 type thermoresistance data characteristics generated by the following formula (UNI-7937 specifications):

$$R = 100 * (1 + 3.90802E-3 * T - 0.5802E-6 * T^2)$$

Westinghouse Non-Proprietary Class 3



AP600 Design
Certification Program
SPES-2 Tests Final
Data Report

WCAP-14310
Rev. 2

Westinghouse Energy Services



Wellington
Non-Proprietary
Class 3

WCAP 14310
Revision 2

AP600 Design Certification Program
SPES-2 Tests Final Data Report

May 1997

